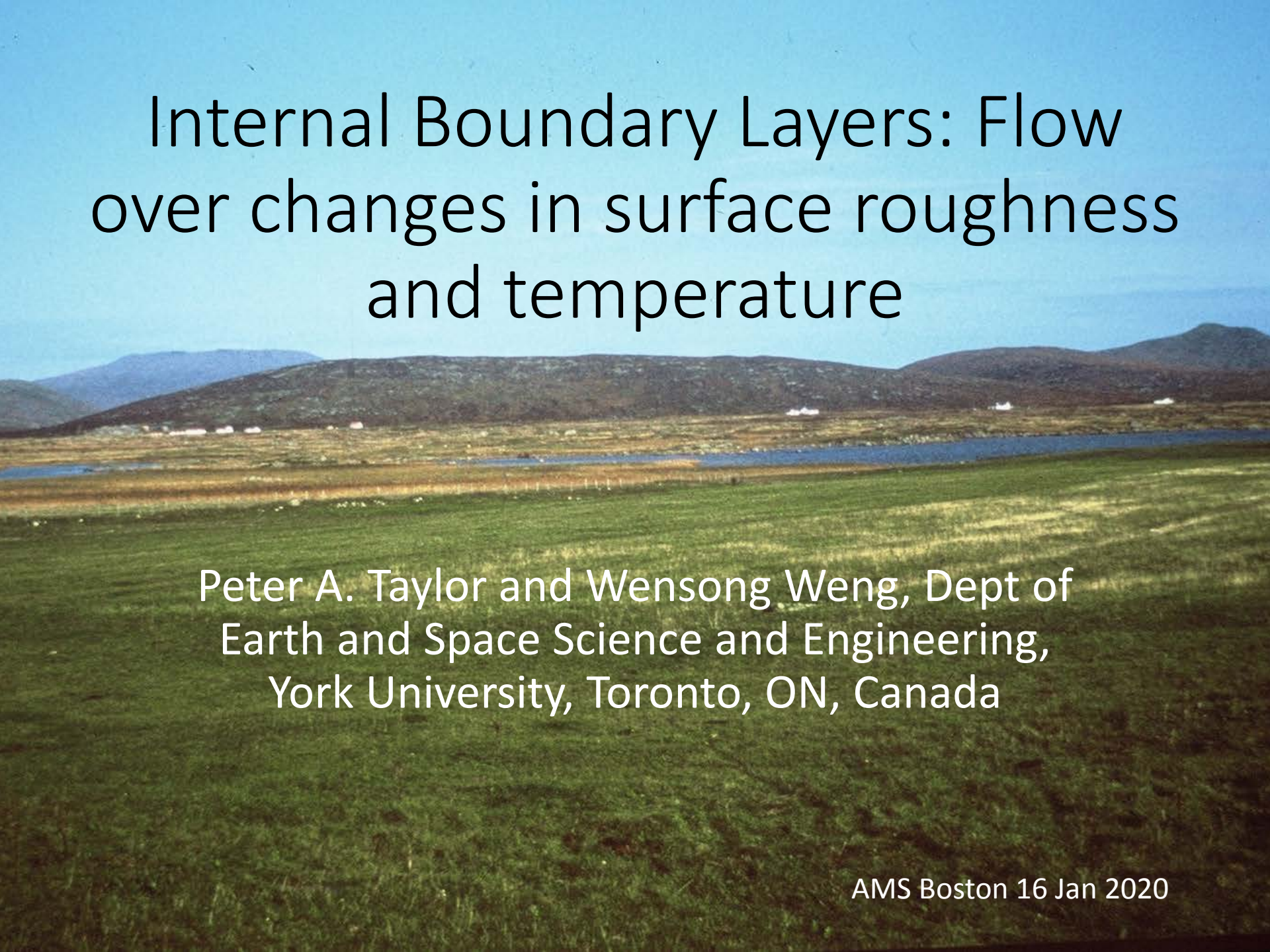


Internal Boundary Layers: Flow over changes in surface roughness and temperature



Peter A. Taylor and Wensong Weng, Dept of Earth and Space Science and Engineering, York University, Toronto, ON, Canada

The Atmospheric Boundary Layer

- Surface layer, constant flux layer, momentum and heat. Turbulence!
- The planetary boundary layer, Coriolis effects. Inversion capped. Generally time dependent.
- Stratification effects, Monin-Obukhov Similarity
- Roughness length and roughness elements
- Horizontal homogeneity, steady state or diurnal cycle.
- Flat terrain and topographic effects
- Radiative flux divergence, clouds and fog.
- We generally live and work in it – many important applications, including surface fluxes and air quality.

Internal boundary layers, $\delta(x)$

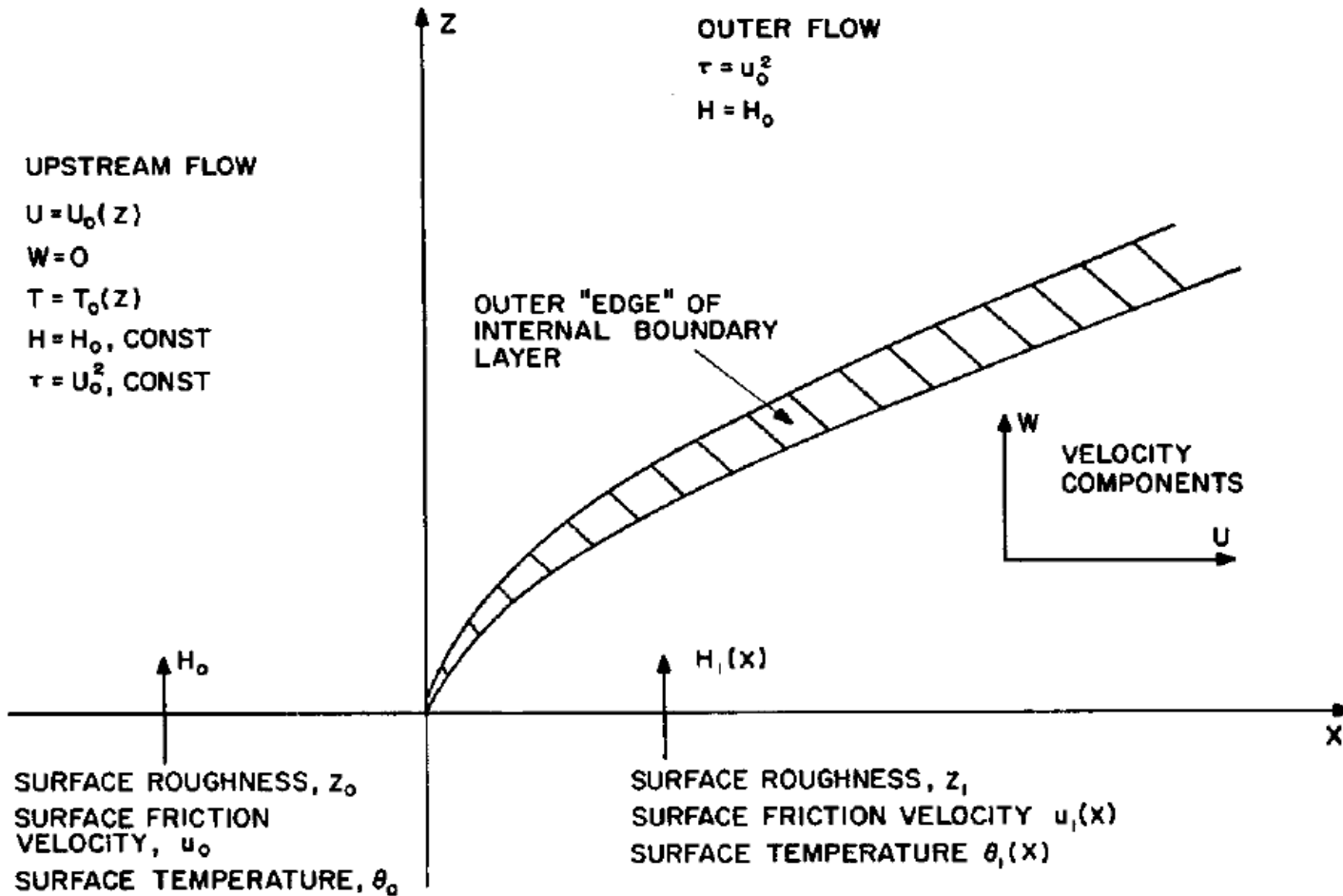


Fig. 1. The internal boundary layer.

Simple log profiles

$M = \ln(z_{01}/z_{02})$, z_{01} is upstream.

$M=4$, rough to smooth

Note plots goes to $U = 0$ so simple log profiles,

$$U = (u^*/k) \ln(z/z_0)$$

Have $U = 0$ at $z = z_0$.

Note $e^4 = 54.6$ and $\log_{10}(54.6) = 1.74$

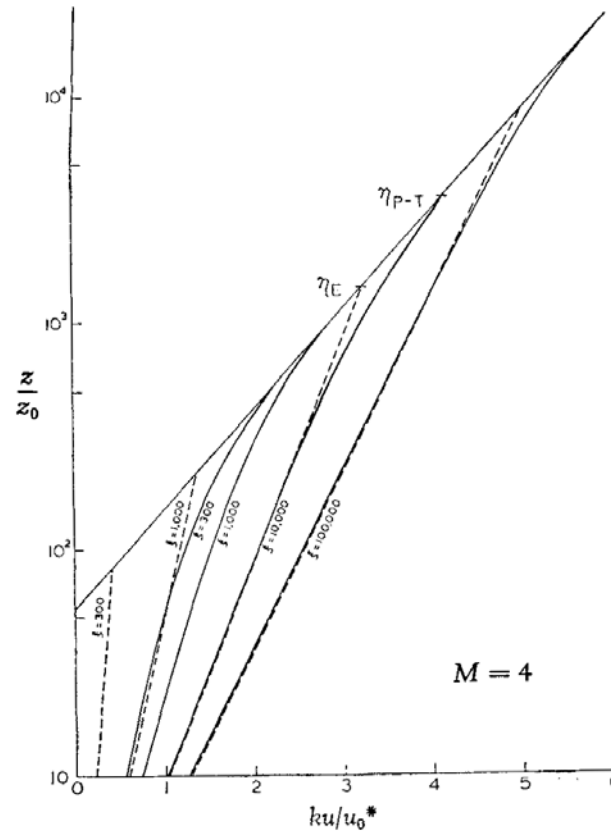


Figure 3. Theoretical wind profiles for air flowing from rough to smooth terrain ($M = 4$).

- Panofsky-Townsend
- - - Elliott

Internal Boundary layers – roughness changes

- In the mid to late 1950s and through the 1960s William P. Elliott, Hans Panofsky, Alan Townsend and others developed models of Internal Boundary Layers (IBLs) developing as air flows over a step change in surface roughness.
- Change of terrain roughness and the wind profile, H. A. Panofsky and A. A. Townsend. QJRMS 1964 Volume, 90, 147-155 : To describe the distribution of wind with height in hydrostatically-neutral air following a change in terrain roughness, a theory is constructed by assuming that only the air below an internal boundary is affected by the change and that air above the boundary is moving with the speed and Reynolds stress that it had upwind of the change of roughness.
- They assumed a u^* profile within the IBL, $u^* = u_1^* [(1 - S) + S z/d]$ where $S = (u_1^* - u_0^*)/u_1^*$, with u_1^* being the upstream value, and d is the IBL depth. Elliott had used a constant u^* and a log profile within the IBL. Both lead to ODEs for $d(x)$ which can be solved numerically.
- Taylor (1969a,b) solved 2D RANS with simple mixing length closure, for surface and planetary boundary layers.

How deep is the IBL? – Savelyev and Taylor, 2005

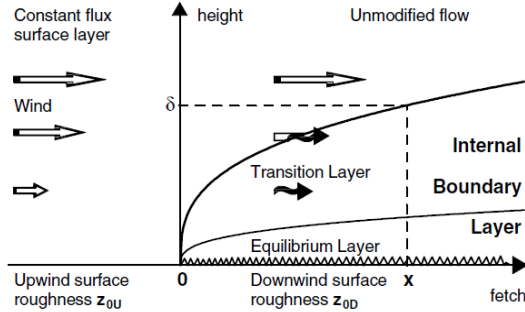


Figure 1. Sketch of a two-dimensional internal boundary layer developing within a constant-flux surface layer after a change in surface conditions. δ is the height of the interface at distance x from a leading edge.

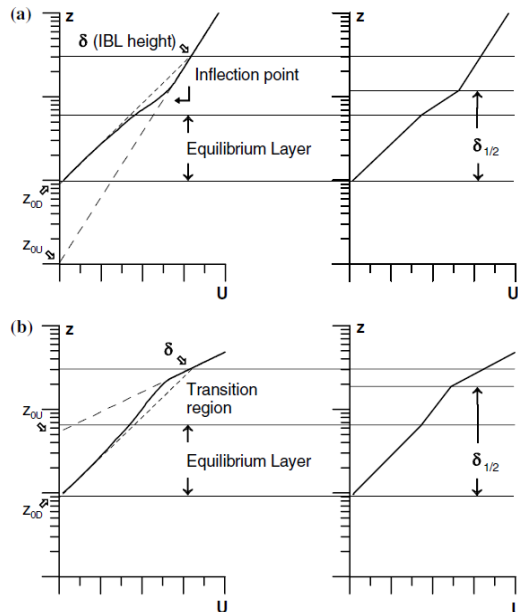


Figure 2. Sketches of the wind speed profile (left panel) at some distance from a leading edge and possible definitions of the IBL height near the inflection point of the profile (right panel); smooth-to-rough (a) and rough-to-smooth (b) transitions.

TABLE I

Short fetch IBL height formulae (in chronological order). IBL height δ and distance from a leading edge x are in metres.

Formula	Author(s)	Notes
$\frac{\delta}{z_{0D}} = (0.75 - 0.03M) \left(\frac{x}{z_{0D}}\right)^{0.8}$	Elliott (1958)	$M = \ln \frac{z_{0D}}{z_{0U}}$
$4\kappa^2 \left(\frac{x}{z_{0U}} - \frac{z_{0D}}{z_{0U}}\right) = \frac{\delta}{z_{0U}} \left[\delta \ln \frac{\delta}{z_{0U}} - 5 + \frac{M}{2} + \frac{4-7M/6-M^2}{\ln(\delta/z_{0D})-1+M/4} + \frac{4+7M/6+M^2/24+M^2/16}{(\ln(\delta/z_{0D})-1+M/4)^2} \right]$ $x_0 = 0$ for $-M \leq 3$ else $4\kappa^2 \frac{z_{0D}}{z_{0U}} e^{M-1} = -\frac{64}{27} - \frac{M}{18} - \frac{88}{27M} + \frac{64}{9M^2}$	Panofsky and Townsend (1964)	z_0 is the surface roughness length, κ is the von Karman const.
$2\kappa^2 x = \delta \ln \frac{\delta}{z_{0D}}$	Townsend (1965)	
$1.73\kappa \frac{x}{z_{0D}} = \frac{\delta}{z_{0D}} (\ln \frac{\delta}{z_{0D}} - 1) - \frac{z_{0D}}{z_{0U}} (\ln \frac{z_{0D}}{z_{0U}} - 1)$	Miyake (1965)	$\delta_0 = \delta(x=0)$
$\kappa^2 x = \delta \frac{\ln \frac{\delta}{z_{0D}} (\ln \frac{\delta}{z_{0D}} + M)}{2 \ln \frac{\delta}{z_{0D}} + M}$	Townsend (1966)	$\kappa^2 x = \frac{\delta \ln \frac{\delta}{z_{0U}} \ln \frac{\delta}{z_{0D}}}{2 \ln \frac{\delta}{z_{0U}} \frac{\delta}{z_{0D}}}$
$\frac{d\delta}{dx} = \kappa^2 \frac{\delta}{z_{0U}} \frac{\ln^2 \frac{\delta}{z_{0D}} + \ln \frac{\delta}{z_{0D}}}{F(\delta) \ln \frac{\delta}{z_{0U}}}$ $F(\delta) = \frac{\delta}{z_{0U}} \ln^2 \frac{\delta}{z_{0D}} - \ln \frac{\delta}{z_{0D}} \left(3 \frac{\delta}{z_{0U}} + \frac{z_{0D}}{z_{0U}} \right) + 4 \left(\frac{\delta}{z_{0U}} - \frac{z_{0D}}{z_{0U}} \right)$ $\delta = f_1 \left(\frac{z_{0D}}{z_{0U}} \right) x^{(0.8+f_2(z_{0U}/z_{0D}))}$	Radikevitch (1971)	$\delta(x=0) = z_{0D}$
$\delta = f_1 \left(\frac{z_{0D}}{z_{0U}} \right) x^{(0.8+f_2(z_{0U}/z_{0D}))}$	Shir (1972)	f_1, f_2 are not given
$1.5\kappa \frac{x}{z_{0U}} = \frac{\delta}{z_{0U}} \left(\ln \frac{\delta}{z_{0U}} - 1 \right)$	Panofsky (1973)	$z_0 = \max(z_{0U}, z_{0D})$
$\frac{\delta}{z_{0D}} = 0.095 \left(\frac{x}{z_{0D}} \right)^{1.03}$	Schofield (1975)	Wind-tunnel data
$0.75\kappa \frac{x}{z_0} = \frac{\delta}{z_0} \left(\ln \frac{\delta}{z_0} - 1 \right) - \frac{z_0}{z_0} \left(\ln \frac{\delta}{z_0} - 1 \right)$	Jackson (1976)	$\delta' = \delta - d_D$ d_D - displacement $z_0' = \sqrt{\frac{z_{0U}^2 + z_{0D}^2}{2}}$ $f_1(M)$
$\frac{\delta}{z_{0U}} = f_1(M) \left(\frac{x}{z_{0D}} \right)^{0.8}$	Andreopoulos and Wood (1982)	was tabulated elsewhere
$\frac{\delta}{z_{0U}} = 0.28 \left(\frac{x}{z_{0D}} \right)^{0.8}$	Wood (1982)	$z_{0U} = \max(z_{0U}, z_{0D})$
$\kappa \frac{x}{z_{0U}} = \frac{\delta}{z_{0U}} \left(\ln \frac{\delta}{z_{0U}} - \ln \frac{z_{0D}}{z_{0U}} - 1 \right) + \frac{z_{0D}}{z_{0U}}$ $\frac{\delta}{z_{0D}} = 0.32 \left(\frac{x}{z_{0D}} \right)^{0.8}$	Raabe (1983)	
$1.25\kappa \frac{x}{z_{0D}} = \frac{\delta}{z_{0D}} \left(\ln \frac{\delta}{z_{0D}} - 1 \right) + 1$	Pendergrass and Aria (1984)	
$2.25\kappa \frac{x}{z_{0U}} = \frac{\delta}{z_{0U}} \left(\ln \frac{\delta}{z_{0U}} - 1 \right)$ $\delta = C\delta^*$ $\delta = 0.09x^{0.8}$	Panofsky and Dutton (1984)	
$\delta \left(\ln \frac{\delta}{z_{0U}} - 1 \right) = 1.25\kappa(1 + 0.1M)x$	Troen et al. (1987)	$C = 0.3$ (constant)
$\frac{\delta}{z_{0D}} = 10.56 \left(\frac{x}{z_{0D}} \right)^{0.33}$ $\frac{d\delta}{dx} = C\kappa \left(1 + \frac{\delta}{x} M \right) \left(\ln \frac{\delta}{z_{0U}} \right)^{-1}$ $\delta \left(\ln \frac{\delta}{z_{0U}} - 1 - C\kappa M \right) = C_{\kappa x}$	WASP model	Data fetch range: 140 - 260 m
	Jegade and Foken (1999)	$M = \ln \frac{z_{0D}}{z_{0U}}$
	Savelyev and Taylor (2001)	
	Cheng and Castro (2002)	
	Equation (23)	$C = \sigma_w/u_* (= 1.25)$
	Equation (26)	$2\delta \left(\ln \frac{\delta}{\sqrt{z_{0U} z_{0D}}} - 1 \right) = x$

Some Field Studies

- R.J Taylor (1962) Field and wind tunnel studies
- Studies on the frozen surface of Lake Mendota (near Madison, Wisconsin) by Charles Stearns, John Kutzbach and Heinz Lettau (1961, 1964) are innovative.
- Their roughness changes were created with 500 bushel baskets in one case (1961) and with the same number of left-over Christmas trees in the other (1964).
- Frank Bradley's (1968) roughness changes were created with metal spikes laid on top of an airport runway and the natural change from grass to the tarmac runway at Jervis Bay, Australia.
- Flow from land to water and vice-versa are an important example, and relevant on many length scales See Smedman et al (1997) for example.

Bradley, E. F.: 1968, 'A Micrometeorological Study of Velocity Profiles and Surface Drag in the Region Modified by a Change in Surface Roughness', *Quart. J. Roy. Meteorol. Soc.* **94**, 361–379.

Smedman, Ann-Sofi et al. "Evolution of stable internal boundary layers over a cold sea." JGR 102, 1091-1099 (1997).

Field Studies

- Stearns and Lettau (1964)

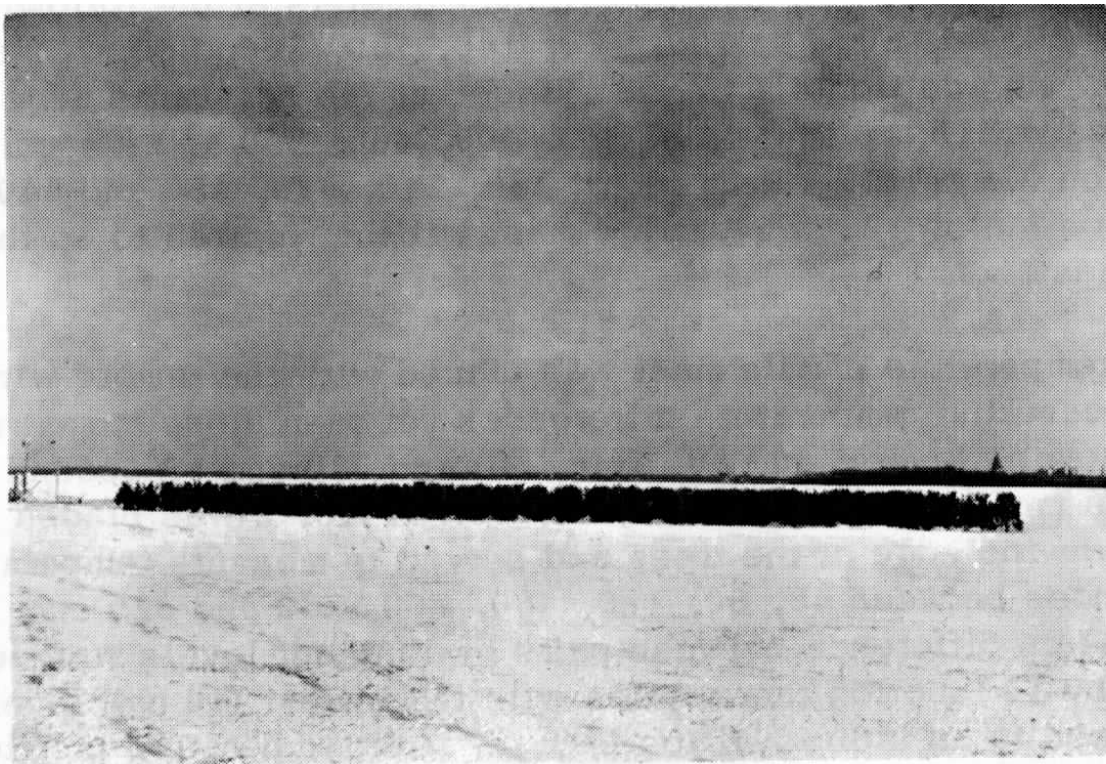
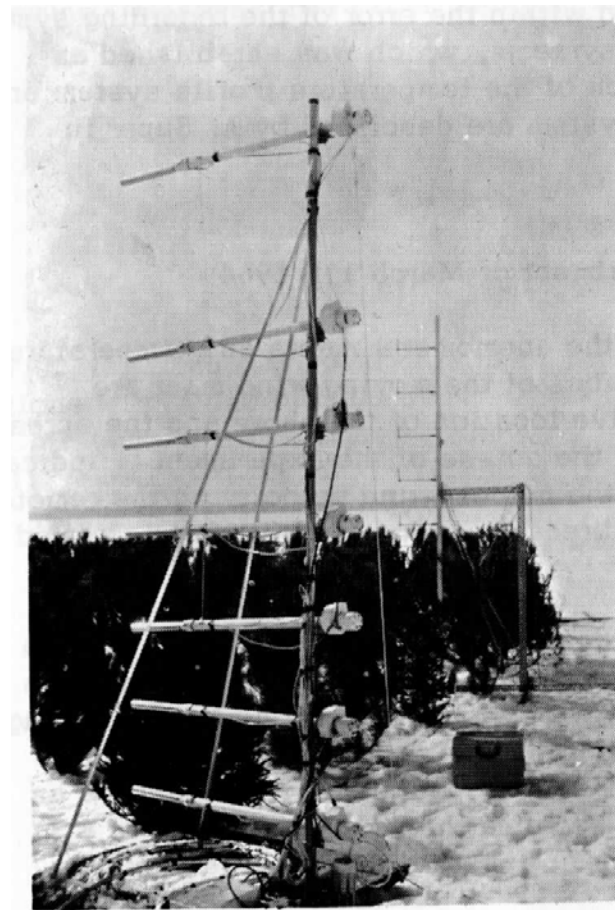


Fig. 1. Christmas Tree "Planted" on the Lake Mendota ice.



Some of my work on Internal boundary layers – flow over changes in surface conditions (roughness and temperature).

Early work –

Taylor, P.A., 1969: On wind and shear stress profiles above a change in surface roughness. *Quart. J. Roy. Met. Soc.*, 95, 77-91;

Taylor, P.A., 1969: The planetary boundary layer above a change in surface roughness. *J. Atmos. Sci.*, 26, 432-440.

Taylor, P.A., 1970: A model of airflow above changes in surface heat flux, temperature and roughness for neutral and unstable conditions. *Boundary-Layer Met.*, 1, 18-39

A more recent addition,

Weng, W., Taylor, P.A. and Salmon, J.R., 2010, A 2-D numerical model of boundary-layer flow over single and multiple surface condition changes, *J. Wind Eng & Industrial Aerodynamics*, 98, 121-132

2D surface boundary layer approximation

x-momentum

$$U \frac{\partial U}{\partial x} + W \frac{\partial U}{\partial z} = \frac{\partial \tau}{\partial z}.$$

Heat flow

$$\rho c_p \left[U \frac{\partial \theta}{\partial x} + W \frac{\partial \theta}{\partial z} \right] = - \frac{\partial H}{\partial z}.$$

Continuity

$$\frac{\partial U}{\partial x} + \frac{\partial W}{\partial z} = 0.$$

Later work with TKE equation and closure.

Closure assumptions for $L < 0$

$$\tau^{1/2} = \frac{k(z + z_i)}{\varphi_M} \frac{\partial U}{\partial z}.$$

$$H = - \rho c_p \frac{k(z + z_i)}{\varphi_H} \tau^{1/2} \frac{\partial \theta}{\partial z},$$

$$\varphi_M = \left[1 - \frac{B(z + z_i)}{L} \right]^{-1/4}$$

$$\varphi_H = \varphi_M^2$$

$$L = - \left(\frac{\rho c_p \theta}{kg} \right) \frac{\tau^{3/2}}{H}.$$

Also need boundary conditions, $x = 0$, $z = 0$, top

From Rider, Phillip and Bradley (1963) - QJRMS
Flow from a dry tarmac runway onto grass, $U_1 = 4\text{ms}^{-1}$

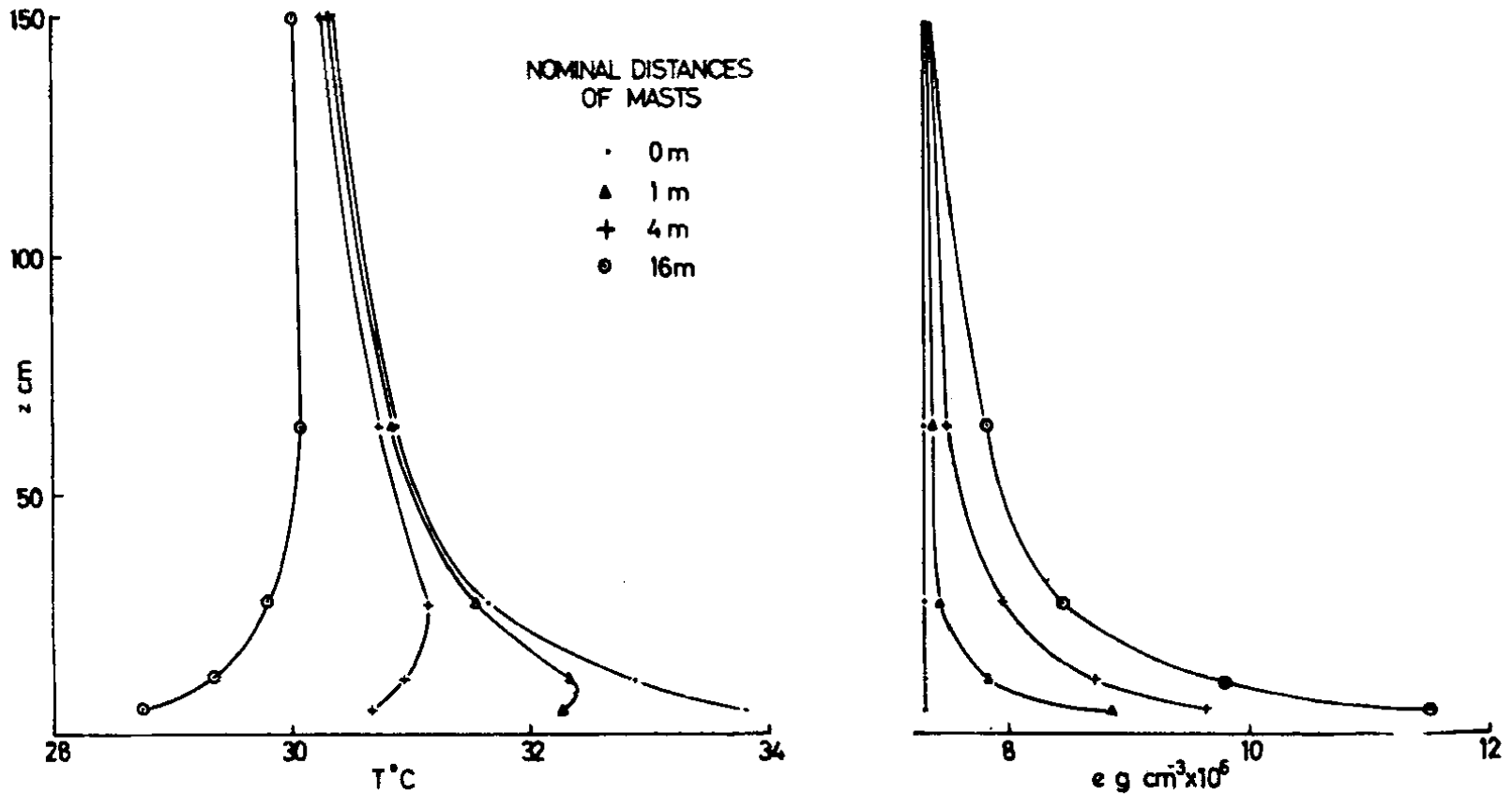


Figure 3. Example of the vertical temperature and humidity profiles (observation No. 7).

Air flow from warm to cool surface. The experimental observations with which the present model (Taylor, 1971) will be compared are those of Rider, Philip and Bradley (1963). Their experiments deal with the case of flow from a dry tarmac surface to a cool grass surface. The upstream surface is relatively smooth and in the experiments the upstream temperature profile is thermally unstable. $Z_1 = 0.0014\text{m}$

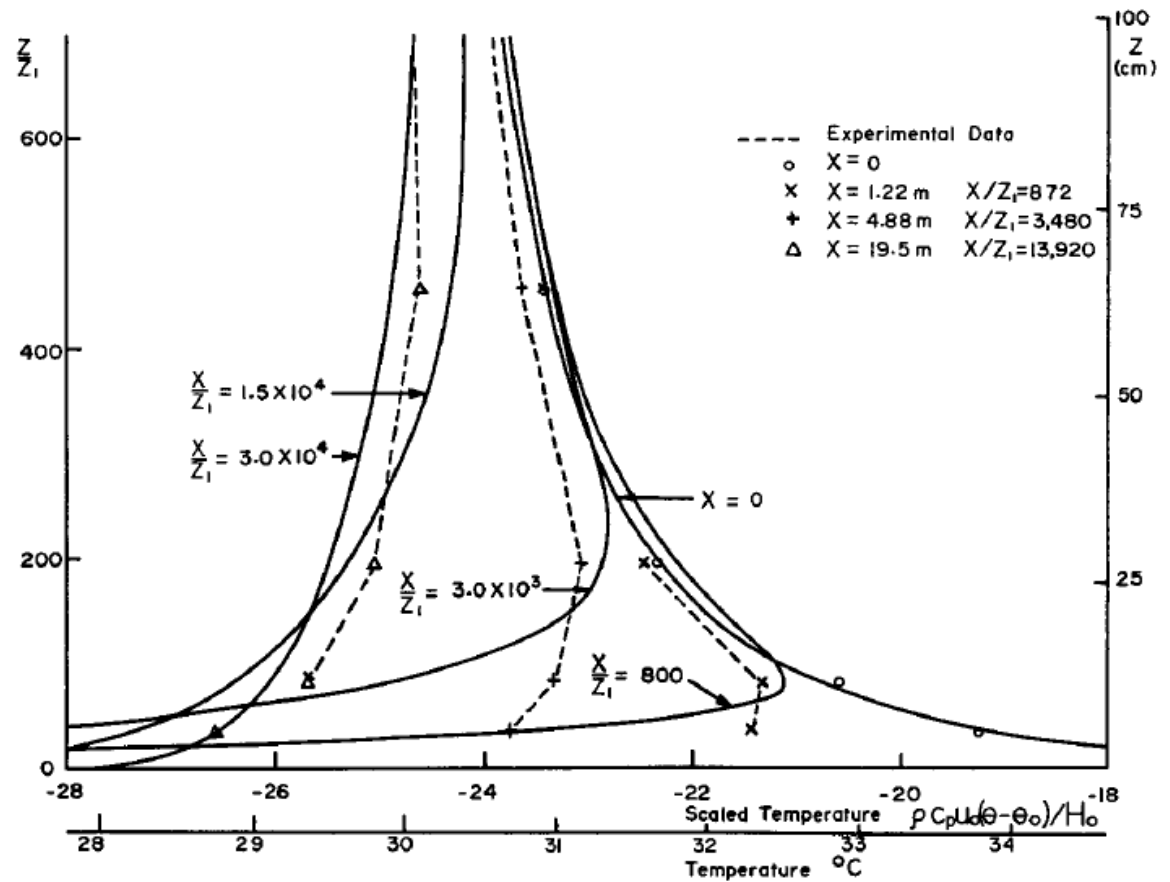


Fig. 15. Temperature profiles, comparison with RPB No. 7.

We need more experimental data!

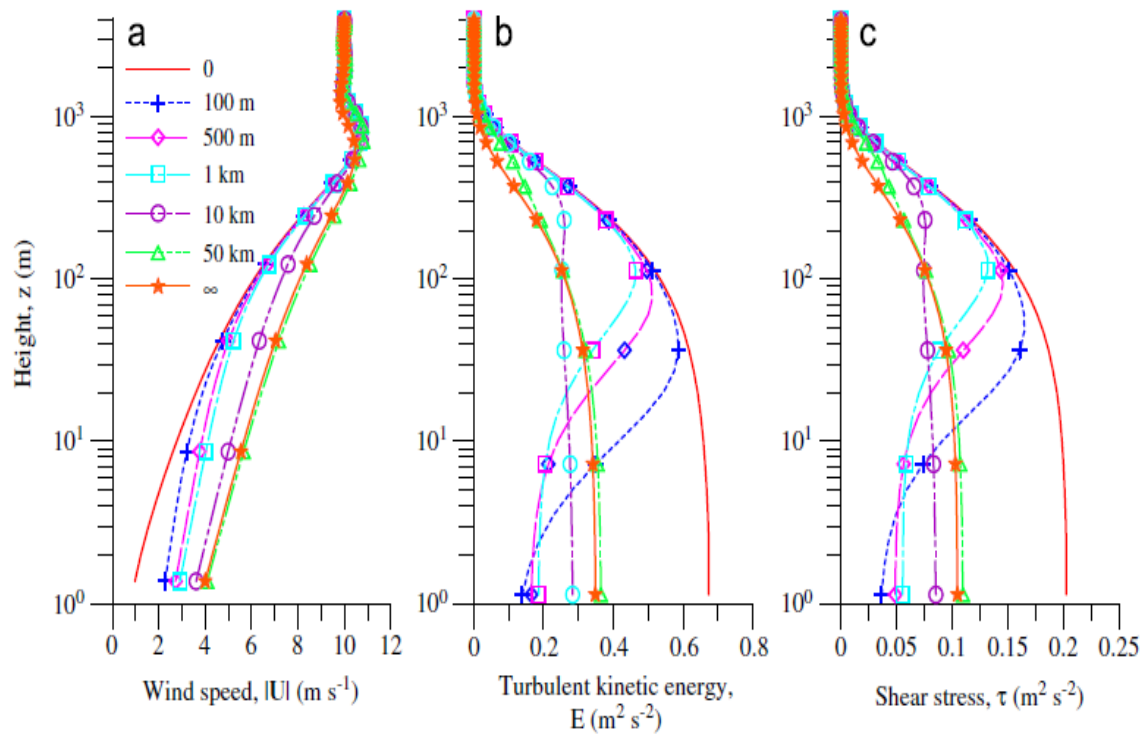


Fig. 4. Vertical profiles at various downwind locations (rough-smooth transition: $z_{01} = 1.0 \text{ m} \rightarrow z_{02} = 0.01 \text{ m}$) from Model A: (a) mean wind speed, (b) turbulent kinetic energy and (c) shear stress. Note that results of the 1-D PBL model run, which corresponds to $z_{02} = 0.01 \text{ m}$, the Coriolis parameter $f = 10^{-4} \text{ s}^{-1}$, geostrophic wind $(U_g, V_g) = (8.70, -4.93) \text{ m s}^{-1}$, neutral thermal stratification and dry air, are marked as $x = \infty$.

W. Weng et al. / J. Wind Eng. Ind. Aerodyn. 98 (2010) 121–132.
 Sample results, PBL with single roughness change, forest to farmland

Current work with Wensong Weng on warm advection fog – warm moist air advected over colder water. The Grand Banks project. Fog Modelling in Nocturnal Boundary Layers (Boundary-Layer and WRF-SCM modelling of marine fog), CMOS 2018 talk. 1-D time dependent and 2-D steady state,

$$\frac{\partial U}{\partial t} = -\frac{\partial \langle uw \rangle}{\partial z} + f(V - V_g)$$

$$\frac{\partial V}{\partial t} = -\frac{\partial \langle vw \rangle}{\partial z} - f(U - U_g)$$

$$\frac{\partial \Theta_l}{\partial t} = -\frac{\partial \langle w\theta_l \rangle}{\partial z} - \frac{\Theta}{T} \left(\frac{1}{c_p \rho} \frac{\partial R_{net}}{\partial z} + \frac{L}{c_p} \frac{\partial G}{\partial z} \right)$$

$$\frac{\partial Q_w}{\partial t} = -\frac{\partial \langle wq_w \rangle}{\partial z} + \frac{\partial G}{\partial z}$$

U, W, u, v, w are velocities, f is Coriolis parameter,

$\Theta_l = \Theta - (\Theta L_v / T c_p) Q_l$ is liquid water potential temperature,

R_{net} is net radiative flux (+ve upwards), Q_w is the total water content ($Q_v + Q_l$), G is

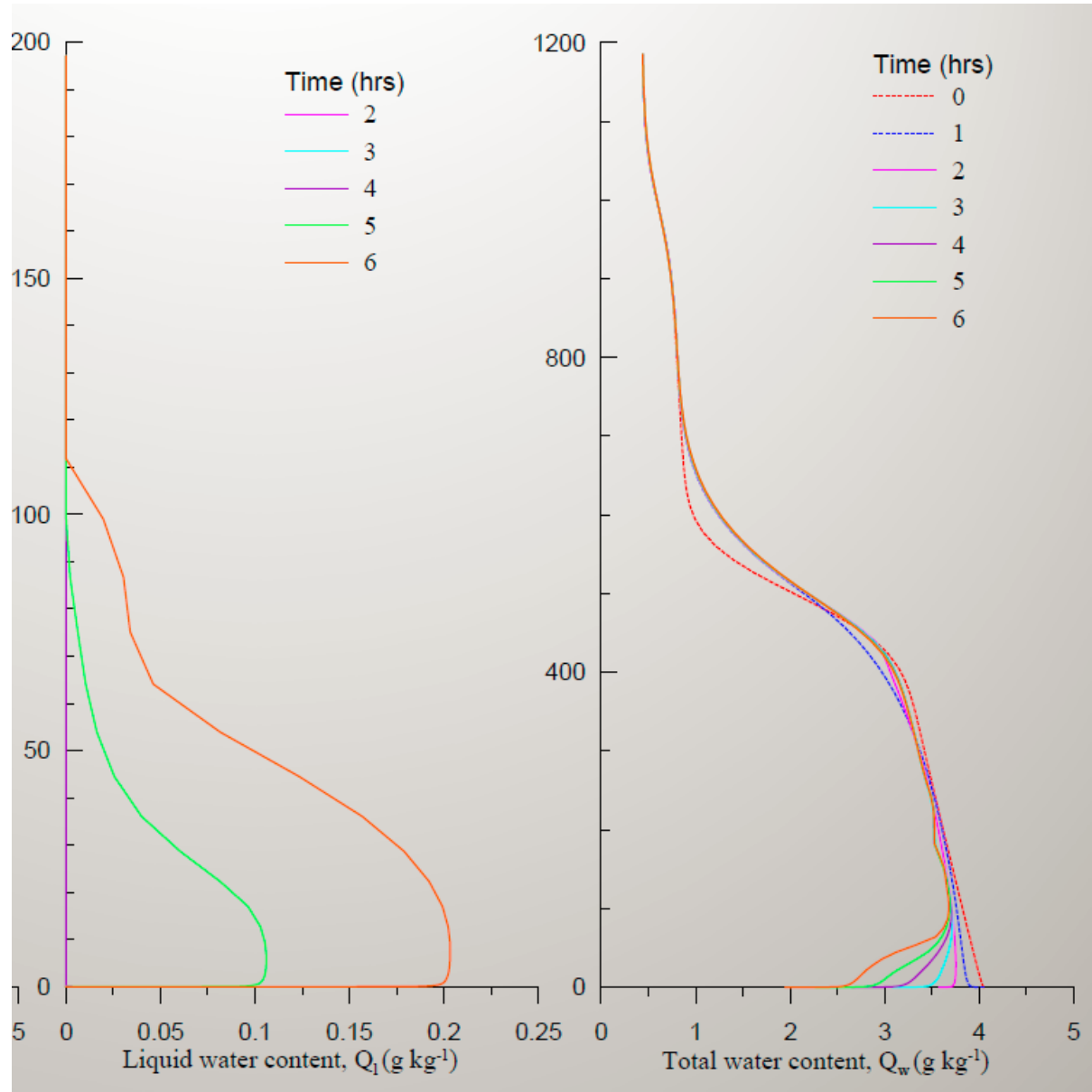
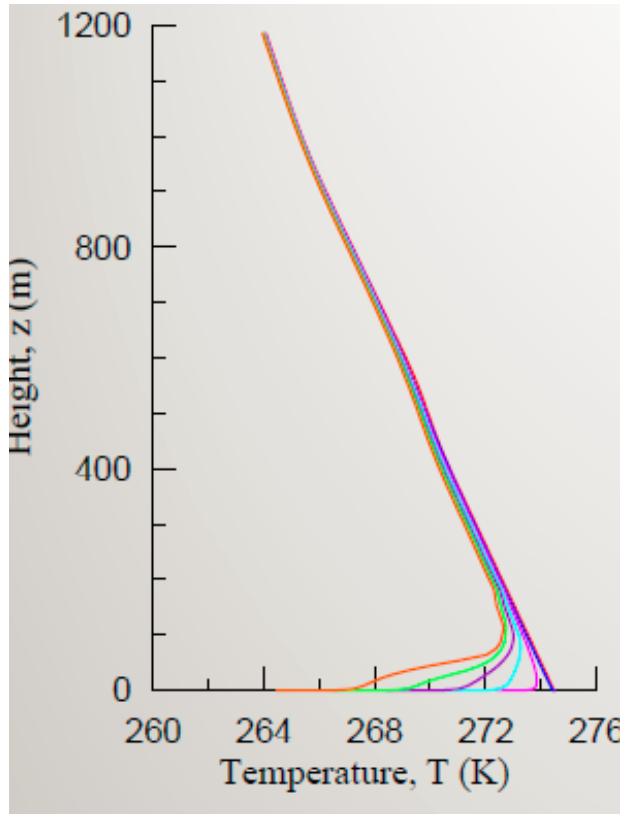
gravitational settling flux of liquid water (+ve

downwards), also in TKE

Equation, $\Theta_v = \Theta(1 + 0.61 Q_v - Q_l)$

Equation, $\Theta_v = \Theta(1 + 0.61 Q_v - Q_l)$

Radiative flux divergence, how important is it? I think it can be – liquid water drops are better absorbers/emitters of long wave radiation than water vapour – leads to convective instability at fog top, or cloudtops, and affects mixing/entrainment.



Sample results – a work in progress. Initial profiles near saturated, then surface is cooled. Upper boundary conditions in LW radiation are a problem. Surface b.c. on liquid water?

Progress has certainly been made over the past 100 years but there are still things to do! In his IBL review, John Garratt (1990) concludes ".... there would seem to be a requirement for an additional comprehensive observational set, perhaps covering a somewhat larger fetch range to encompass the transition between the small-scale problem and that at the mesoscale." There have been some field studies in the almost 30 years since then, including Jegede and Foken (1999) as part of the LINEX project in Germany, Pires et al (2015) at Alcantara, Brazil, and a small project at the Wind Energy Institute on Prince Edward Island, Canada - Miller and Taylor (2016). I would second John's opinion, and maybe look for more than one extra data set. Remote sensing with Doppler lidars can help but for high resolutions turbulence and temperature fields we need basic in situ measurements from multiple masts or tethered balloons. A fundamental IBL study could be a fun, basic science project to provide the data needed to validate and compare models and ideas, **lets find the support and do it!**

Garratt, J.R., *Boundary-Layer Meteorol.* (1990) 50: 171-203. The internal boundary layer — A review. <https://doi.org/10.1007/BF00120524>

Jegede, O. & Foken, Thomas. (1999). A Study of the Internal Boundary Layer due to a Roughness Change in Neutral Conditions Observed During the LINEX Field Campaigns. *Theoretical and Applied Climatology*. 62. 31-41. 10.1007/s007040050072.